NaCl particle interaction with 193-nm light: Ultraviolet photofragmentation and nanoparticle production

Jong Hyun Choi
Mechanical Engineering Department, University of California, Berkeley, California 94720

Christopher B. Stipe
Mechanical Engineering Department, Seattle University, Seattle, Washington 98122

Catherine P. Koshland
School of Public Health, University of California, Berkeley, California 94720

Robert F. Sawyer
Mechanical Engineering Department, University of California, Berkeley, California 94720

Donald Lucas[a)]
Environmental Energy Technologies Division, Lawrence Berkeley National Laboratory, Berkeley, California 94720

(Received 6 December 2004; accepted 16 May 2005; published online 27 June 2005)

The interaction of nanoscale NaCl particles with 193-nm photons is studied to better understand particle disintegration and production by ultraviolet photofragmentation. The particles are irradiated in a constrained air stream with laser fluences from 0.08 to 0.23 J/cm^2 with single and multiple pulses striking the particles. The resulting particle size distributions are measured with a scanning mobility particle sizer and the morphology is analyzed qualitatively by scanning electron microscopy (SEM). Photofragmentation of NaCl particles at 193 nm produces gas-phase species as well as small solid-phase fragments without significantly heating the particles or creating a plasma. The irradiated particles have a mean diameter from 20 to 55 nm (depending on the photon energy) and a number concentration an order of magnitude higher than the 118-nm mean diameter nonirradiated particles. The SEM images before and after 193-nm irradiation reveal that the irradiated particles are less fractal and more spherical. © *2005 American Institute of Physics*. [DOI: 10.1063/1.1948511]

I. INTRODUCTION

The interaction of laser light with particles is of interest to both basic and applied scientists and engineers. Fundamental properties of particles, including the chemical composition and species concentration, can be measured through particle disintegration in instruments such as the aerosol time-of-flight mass spectrometer (ATOFMS).[1] The signal measured in this technique depends on the species type and concentration after the disintegration process. The disintegration of nanoparticles is not well understood, as it is a complex phenomenon that depends on numerous factors including laser wavelength, pulse duration and energy, and the optical properties of the nanoparticles. Understanding laser interactions with particles would also benefit nanoparticle production techniques, since the size, morphology, and number concentration of the particles can also be manipulated with laser irradiation.[2–5]

We previously conducted a series of experiments on the interaction between UV light and combustion-generated soot particles.[6–8] When soot particles are photofragmented by 193-nm photons, photolyzed carbon atoms are electronically excited and emit fluorescence at 248 nm. The atomic emission can be used to monitor soot concentrations from combustion systems. The particle size distributions before and after laser irradiation revealed that the mean diameter and number concentration of the photofragmented soot particles could be controlled by varying laser parameters. However, in this system carbon oxidation plays a pivotal role in determining the final particle size, since many of the species produced by photofragmentation react with the surrounding air to form gas-phase compounds. As the laser fluence irradiating the soot particles increased, a greater proportion of the original particle mass was lost due to oxidation. Electron microscope analysis also revealed that 193-nm laser irradiation drastically modifies the microstructure of carbonaceous particles.

Here, we investigate the interaction of 193-nm light with NaCl particles. There are several advantages in using sodium chloride; the chemical composition, molecular structure, optical, and material properties are well known,[9,10] especially compared to combustion-generated soot, and it does not significantly oxidize, which makes nucleation and agglomeration of the photofragmented particles easier to understand. The original NaCl particles are fractal agglomerates composed of nearly spherical primary particles, similar to that for soot particles.

There are previous studies on laser irradiation of NaCl particles and surfaces.[11–15] Dickinson and co-workers[13,15] investigated NaCl surface interactions with 248-nm photons. Since NaCl is a wide-band-gap material, the bulk surface is not readily photofragmented by these photons. However,

[a)]Electronic mail: d_lucas@lbl.gov

they showed that laser ablation could be promoted through an incubation process, where the laser-surface interaction gradually increases when absorption by lattice defects promotes electrons to a conduction band. Laser ablation at 157 nm by Dyer *et al.*[11] produced detectable amounts of NaCl from the surface approximately at 0.08 J/cm^2, and they attributed this mainly to photolytic decomposition. However, surface heating is not negligible at higher fluences as a plasma plume can be formed, leading to conductive and radiative heat transfer from the hot gas. These studies focused on material removal of the bulk surface rather than on the behavior of the ablated materials.

Photofragmentation-fluorescence measurement techniques use excimer lasers to generate species that subsequently fluoresce without producing much optical noise. Gas-phase NaCl molecules efficiently absorb 193-nm light, producing sodium fluorescence at the 589-nm doublet (Na *D* line) through bond dissociation and electronic excitation. The detection limit is at sub-parts per billion (ppb) levels.[16–19] Nunez and Omenetto[14] employed 193-nm photofragmentation to measure this fluorescence from NaCl and other sodium-containing aerosols. They found that the time to reach the maximum fluorescence signal strongly depends on the chemical composition of the particle and the photon energy incident on the particle surface. In addition, the time needed to produce gas-phase species increased with increasing particle diameters.

The purpose of the present study is to understand the effects of UV photofragmentation on the size distribution and morphology of NaCl particles. Here, we investigate (1) the particle disintegration process and (2) the mechanisms involved in creating a new mode of particles. Ultimately, this work along with our previous soot studies will contribute to a better understanding of particle disintegration process for laser-based particle measurements and could lead to methods for producing nanoparticles.

II. EXPERIMENT

We used two particle sources to achieve two different size distributions of NaCl particles. The schematic diagrams in Fig. 1 show the two sources. In Fig. 1(a), air at 5.8 standard liters per minute (slpm) is supplied to a three-jet Collision nebulizer (BGI, CN-24), generating droplets from a 0.1*M* solution of NaCl in de-ionized water. The droplets pass through a diffusion dryer (TSI, 3062), leaving solid-phase NaCl particles. Approximately 0.22 slpm of this particle-laden flow is diluted with air to achieve a total flow rate of 0.3 slpm. These particles have a polydisperse distribution with a mean diameter of 118 nm (geometric standard deviation of 1.9). Figure 1(b) shows the second source that produces NaCl particles through evaporation–condensation in a tube furnace (Lindberg/Blue, TF55030A-1), similar to the particle generator developed by Scheibel and Porstendorfer.[20] Air at 12.2 slpm travels through a quartz tube where the salt evaporates at 800 °C. The tube is 60 cm in length and 2 mm in thickness. The NaCl vapors in the air stream condense to form particles in the water-cooled region after exiting the oven. Without any dilution 2 slpm of this

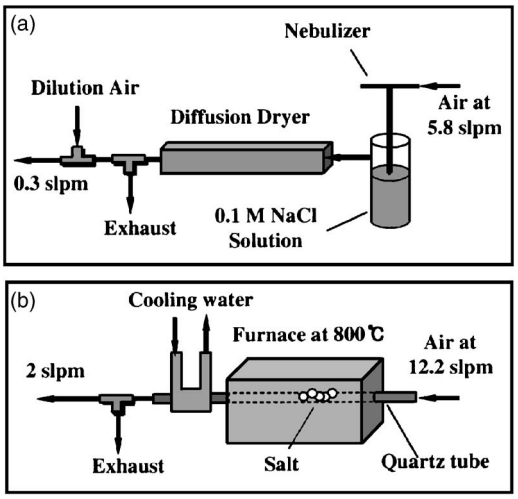

FIG. 1. NaCl particle sources—nebulizer and furnace systems. (a) Nebulizer system. (b) Furnace system.

flow goes to the laser interrogation region. This condition produces polydisperse particles with a mean diameter of 26 nm (geometric standard deviation of 1.4).

Figure 2 shows the laser and measurement systems. An ArF excimer laser (Lambda Physik, LPX 210i) generates 20-ns pulses of 193-nm photons. The laser beam is mildly focused by a 3.8-cm-diameter, 25-cm focal length, planoconvex lens into a $1\times1\times4$-cm^3 quartz cuvette that constrains the particle-laden flow. The cuvette is a standard 1-cm path length UV/Vis absorption cell, with the end removed for flow-through operation. The beam-spot size at the surface of the quartz cell is 10 mm in width by 4 mm in height. Laser energy is measured with a Gentec Joulemeter and corrected for ~20% absorption and reflection of the cuvette. Laser fluences from 0.08 to 0.23 J/cm^2 at repetition rates of 10, 50, and 100 Hz are used.

A scanning mobility particle sizer (SMPS) measures the particle size distributions before and after laser irradiation. The SMPS consists of a differential mobility analyzer (DMA, TSI 3071A) and a condensation particle counter (CPC, TSI 3025A). In this work, we present the size distributions in a normalized format ($d\text{Number}/d\log D_p$) for allowing the distributions to be compared regardless of the

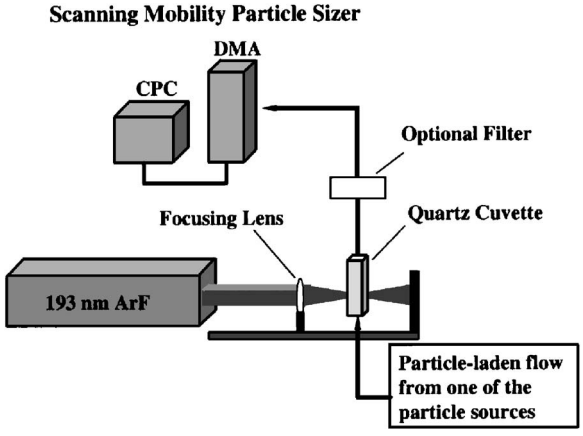

FIG. 2. Laser and measurement system for NaCl fragmentation.

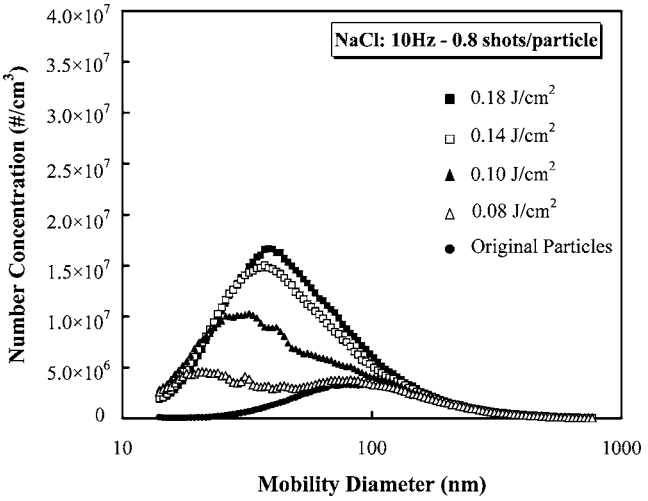

FIG. 3. Size distributions of NaCl particles photofragmented at fluences of 0.08–0.18 J/cm^2 by 193-nm photons at 10 Hz (0.8 shots/particle). The nonirradiated original particle size distribution from the nebulizer system is shown in black-filled circles.

channel resolution, while the total concentrations are calculated by summation of the particle number density in each channel. This is a standard representation of aerosol particle distributions using a SMPS.[21] The details of SMPS measurements are reported in previous work.[7] The uncertainty in the size distribution measurements in the present study is estimated to be less than 15%. While the correlation between the actual particle size and the electric mobility diameter measured by SMPS has received attention,[22] we do not convert the particle mobility diameter in this work.

JEOL 6300 scanning electron microscope (SEM) is used to visualize the microstructure of the NaCl particles. A 47 -mm-diameter Whatman Anodisc membrane filter with a pore size of 20 nm is placed between the cuvette and SMPS to capture the particles before analysis in the SEM. The particles on the filter are coated with a Au/Pt alloy to enhance their conductivity.

III. RESULTS

Figure 3 presents the size distributions of the NaCl particles as a function of laser fluence from 0 to 0.18 J/cm^2 at a laser repetition rate of 10 Hz. The original, nonirradiated particles produced by the nebulizer system have a mean diameter of 118 nm, a number concentration of 2.2×10^6 cm^{-3}, and a volume concentration of 7.1×10^{12} nm^3/cm^3 ($\sim$7 ppb). At a laser repetition rate of 10 Hz, approximately 80% of the particles are hit by a laser pulse while flowing through the quartz cuvette. Photofragmentation at 0.08 J/cm^2 produces a bimodal size distribution with a new small mode of particles whose mean diameter is approximately 20 nm. As the fluence increases to 0.18 J/cm^2, the mean diameter of the peak created by photofragmentation increases to 40 nm and the total number concentration increases from 4.1×10^6 to 1.0×10^7 cm^{-3}. The volume concentration remains constant within 8% of the volume concentration of the nonirradiated particles. Table I shows pertinent data for single and multiple shot experiments.

TABLE I. Data for single and multiple shot photofragmentations of NaCl (from the nebulizer) and soot particles. Note that the total volume of the NaCl particles is conserved at 7.1×10^{12} nm^3/cm^3, while the soot has decreasing volume concentrations of 8.6×10^{12}, 5.0×10^{12}, and 3.9×10^{11} nm^3/cm^3 for 0, 20, and 100 Hz, respectively.

Particles	Fluence (J/cm^2)	Mean diameter (nm)	Number concentration (cm^{-3})
NaCl	0.00	118	2.2×10^6
10 Hz	0.08	20	4.1×10^6
	0.10	30	7.1×10^6
	0.14	37	9.4×10^6
	0.18	39	1.0×10^7
100 Hz	0.08	27	7.9×10^6
	0.10	33	1.1×10^7
	0.14	43	1.5×10^7
	0.18	55	1.8×10^7
Soot	0.00	265	4.5×10^5
20 Hz	0.18	48	1.1×10^7
100 Hz	0.18	21	4.2×10^6

The damage threshold of the quartz cuvette for 193-nm light is approximately 0.3 J/cm^2. Thus, the total energy illuminating the particles is increased by increasing the laser repetition rate instead of further increasing the laser fluence. The size distributions of the photofragmented NaCl particles at 100 Hz are shown in Fig. 4(a). At 100 Hz, eight laser shots strike each particle on average while traveling through the laser probe volume. The original, nonirradiated particles are the same as in the 10-Hz case and the same range of laser fluences is used. The mean diameter of the newly created peak increases from 27 to 55 nm, and the number concentration increases from 7.9×10^6 to 1.8×10^7 cm^{-3}. Again, the volume concentration is preserved as it varies by less than 8% from the original volume concentration of the particles.

The tail of the size distributions from 100 to 1000 nm is used as an indication of the total volume concentration, since the large particles account for most of the total particle volume or mass. Figure 4(b), using the same data in Fig. 4(a), shows the change in the photofragmented particle distributions more clearly in the range of 100–500 nm. For the particles larger than 200 nm, the number concentration is highest for the nonirradiated particles and decreases with increasing laser fluence. Note that a slight decrease in the number concentration of the large particles can produce a large number of small particles; for example, a 1-μm particle has the same volume as approximately 15 000 particles with a diameter of 40 nm. This suggests that the large number of new small particles can be generated from the disintegration of the larger particles originally in the flow.

SEM images in Fig. 5 show the effects of UV irradiation on the NaCl particle morphology. Figure 5(a) shows that the original particles from the nebulizer system have a fractal structure composed of nearly spherical primary particles with a diameter of approximately 40 nm. When compared with soot in our previous study,[7] the original NaCl particles have a similar fractal dimension. The NaCl particles irradiated at 0.16 J/cm^2 and 50 Hz in Fig. 5(b) have a large number of smaller and more spherical particles, similar to what was observed with soot particles.

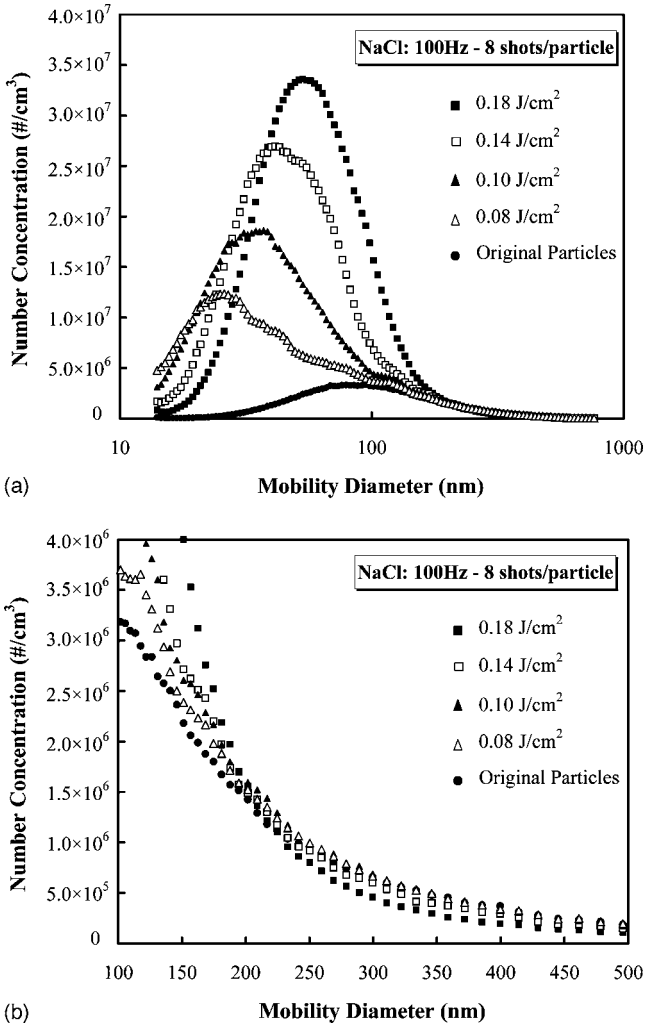

FIG. 4. (a): Size distributions of NaCl particles photofragmented at fluences from 0.08 to 0.18 J/cm^2 by 193-nm photons at 100 Hz (8 shots/particle). The original particle size distribution and the laser fluences applied are the same as the previous 10-Hz case. (b): The enlarged size distributions for the range of 100–500 nm in diameter.

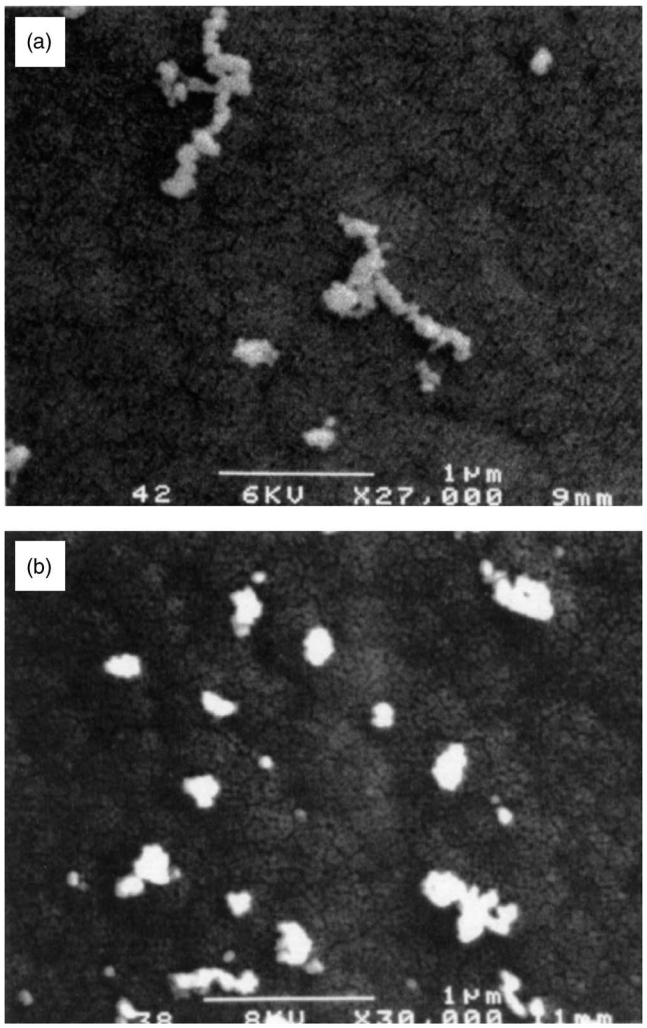

FIG. 5. SEM images of nonirradiated and irradiated NaCl particles. (a) Nonirradiated NaCl Particles from the nebulizer system. (b) NaCl particles irradiated at 0.16 J/cm^2, 50 Hz.

In Fig. 6, the NaCl particles are compared with our previous soot study.[7] The polydisperse agglomerated original soot particles have a mean diameter of 265 nm, a number concentration of 4.5×10^5 cm^{-3}, and a volume concentration of 8.6×10^{12} nm^3/cm^3. The number concentration of the nonirradiated soot particles is smaller than that of the original NaCl particles while the total volume concentration is comparable. Both NaCl and soot particles are irradiated at 0.18 J/cm^2. When the particles are irradiated by single shots (10 and 20 Hz), the size distributions of the photofragmented soot and NaCl particles are qualitatively similar; a new peak with a mean diameter near 40 nm and a number concentration an order of magnitude higher. However, photofragmentation by eight laser pulses (100 Hz) produces completely different size distributions for NaCl and soot particles. The NaCl particles irradiated by multiple laser pulses have a peak with a larger mean diameter and higher concentration than those irradiated by a single shot. In the soot case, the mean diameter and the number concentration decrease with an increasing laser repetition rate. As discussed earlier, the volume concentration of the photofragmented NaCl particles is conserved over all conditions. The volume concentration of the soot particles irradiated by multiple shots decreases by approximately 90%, and there are virtually no particles larger than 100 nm. The loss of soot volume is attributed mainly to the oxidation of gas-phase species released from the soot surface during the disintegration process.

Figure 7 shows the NaCl particles generated in the furnace system. Nonirradiated particles have a mean diameter of 26 nm, a number concentration of 1.4×10^7 cm^{-3}, and a volume concentration of 1.9×10^{11} nm^3/cm^3. The mean diameter is close to the primary particle size of the NaCl particles from the nebulizer system and the number concentration is about an order of magnitude higher. The flow rate through the 1-cm^2 quartz cell is faster at 2 slpm, resulting in 0.8 shots per particle at 50 Hz. The size distributions of the irradiated particles are very similar to the original, nonirradiated distribution. Note that the total volume of the NaCl particles with a mean diameter of 26 nm is an order of magnitude smaller than that of the particles from the nebulizer ($\sim$118 nm). In addition, the absorption efficiency of 193 -nm photons by the smaller NaCl particles from the oven is more than an order of magnitude larger based on Mie scat-

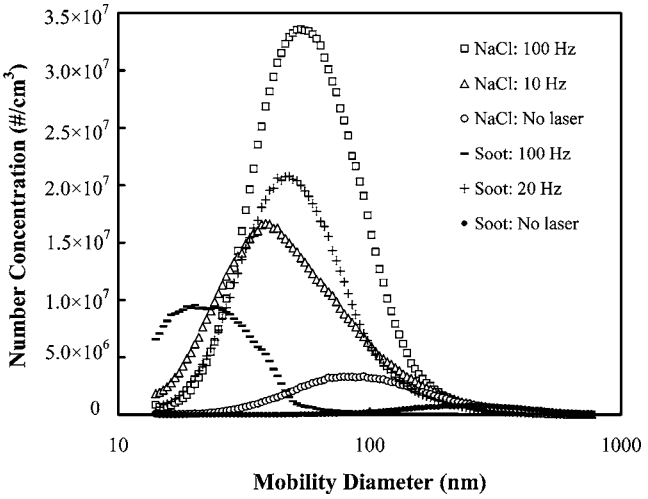

FIG. 6. Size distributions of NaCl and soot particles photofragmented at 0.18 J/cm^2 by 193-nm photons. The size distributions of soot particles are from Ref. 7. NaCl and soot particles at 100 Hz are photofragmented by eight laser pulses while NaCl at 10 Hz and soot at 20 Hz are hit by approximately single laser pulse. The original particles are shown in open and filled circles for NaCl and soot particles, respectively.

tering calculation.[23] Thus, the number of available photons per each atom (photon/atom ratio) is also much higher for the particles with a mean diameter of 26 nm. The photon-to-atom ratio is more relevant to interpret the physical process involved in laser-particle interactions than the laser fluence often used in describing laser-bulk surface interactions. At the same laser fluence, a majority of the particles from the oven are likely vaporized while only a fraction of the particles from the nebulizer is converted into gas-phase species. The resulting size distributions are similar to the original distribution since the condensation condition is similar to the situation where the particles are originally formed in the cooled region after the furnace. After the particles are converted into gas-phase atoms and molecules by laser irradiation, the species form a self-preserving size distribution by nucleation and agglomeration, which is analogous to the process that the species experience at the furnace exit. If the particles were not completely vaporized, the distribution of the irradiated particles would be different from that of the original particles, as seen in Figs. 3 and 4, where the larger particles are not completely vaporized by the laser. Laser-particle interactions appear different and distinct from laser-bulk solid interactions; these differences can be exploited to produce nanoparticles with different properties than those formed from laser ablation of solids.

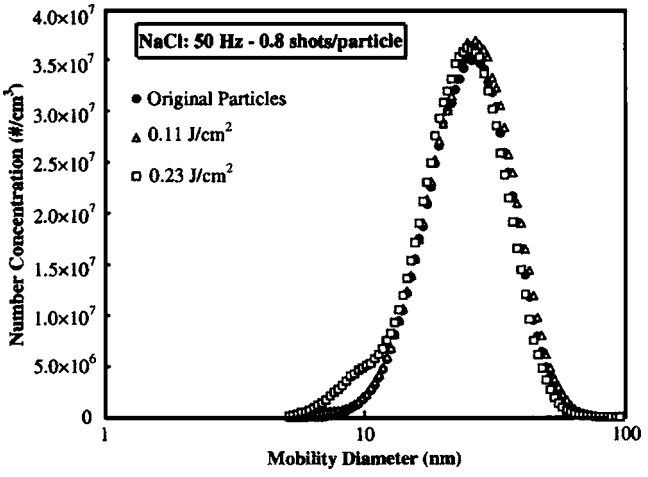

FIG. 7. Size distributions of NaCl particles photofragmented for fluences of 0.11 and 0.23 J/cm^2 by 193-nm photons at 50 Hz. The original particles shown in filled circle are generated from the furnace system. Laser irradiation at 50 Hz of 2-slpm flow in the cuvette makes 0.8 shots per particle.

IV. DISCUSSION

A. UV photofragmentation

In gas phase, NaCl molecules can absorb 193-nm photons, leading directly to their dissociation.[18] Solid NaCl has an ionic crystal structure with an 830-kJ/mol energy difference between the valence and conduction bands, so a 193-nm photon (620 kJ/mol) cannot directly excite an electron to the conduction band. The surface and lowest bulk exciton bands for NaCl lie approximately at 662 and 758 kJ/mol, respectively.[24–26] However, electronic excitation for NaCl or other wide-band-gap alkali halide insulators is often achieved through coherent two (or more) photon absorption process.[27] The electronically excited atoms, molecules, and ions then dissociate from the surface that can be interpreted with the Menzel–Gomer–Redhead (MGR) scenario of desorption induced by electronic transitions (DIET).[28] Lattice defects, such as foreign atoms or vacancies, open another pathway for electronic excitation with photons of sub-band-gap energy. The sequential two-photon absorption via intermediate defect states promotes electronic excitation and subsequent material decomposition. For instance, contamination of hydroxyl ions in NaCl crystals provides an absorption band peaking at 192 nm that may serve as an intermediate state in multiphoton absorption process of NaCl.[29]

Multiphoton absorption of 193-nm photons likely leads to particle disintegration through a photochemical bond breaking process since the overall thermalization of the excitation energy is slow;[27] the electronically excited ($\sim 10^{-15}$ s) species overcome long-range attraction by gaining kinetic energy from short-range repulsion during the vibrational period ($\sim 10^{-13}$ s). Thus, the overall species ejection time scale is approximately 10^{-12} s while relaxation from the interband electronic excitations in nonmetal insulators is much longer, typically, 10^{-12}–10^{-6} s.[27] The bond-broken species are ejected in a few picoseconds due to the increase of specific volume, forming an outgoing shock wave.[30] Nanoscale particles are more vulnerable to photodecomposition than a bulk solid due to their high surface-to-volume ratio. Li *et al.*[31] observed neutral atoms ejected from alkali halide nanocrystals irradiated by 193-nm photons with a photofragmentation quantum yield near unity, where the incident photon energy nearly matches the surface exciton band[25,32] below the bulk absorption edge.

The 193-nm laser irradiation does not significantly increase the thermal energy of the particles as we observe no blackbody-type radiation associated with particle heating or plasma formation[7,8,33,34] from different particles, including NaCl, soot, polystyrene, and gold. The sodium *D* line was observed (not shown here) with a signal-to-noise ratio of

approximately 15 in the photofragmentation-fluorescence measurement of NaCl particles at fluences above 0.3 J/cm^2. If the particles were heated by the laser pulses (e.g., to 3000 K), thermal emission peaking at 1 μm should be observed. When we replaced the excimer laser with a frequency-doubled Nd:YAG (yttrium aluminium garnet) laser at 532 nm at the same fluence, the particles exhibited long lifetime broadband incandescence. This experimental result indicates that particle interaction with 193-nm photons is primarily photochemical while visible photons significantly increase the particle temperature, consistent with other studies.[35–38] Michelson[37] showed that 532-nm laser irradiation predominantly heats soot particles, but at high fluence conditions nonthermal desorption of neutral atoms and molecules from the particle surface can occur through electronic excitation and in turn decrease the particle size. Srinivasan[39] found that photochemical component becomes more important as the laser wavelength decreases and concluded that photochemical decomposition dominates at 193 nm. In addition, we observed that the 193-nm pulses photofragment nanoparticles with a quantum efficiency near unity.[33] It is very difficult evaluating the exact fraction of the absorbed photons that are converted to thermal energy since the majority of the photons are used for photochemical disintegration of the NaCl particles, and the relevant photophysical processes are not well understood.[40] Oman and Garrett[41] roughly estimated the temperature increase of a graphite surface irradiated at 193 nm to be approximately 160 K. If we assume that the temperature of the NaCl particles increases by 200 K after irradiation, a simple calculation of radiation and conduction shows that particle cooling is terminated in 130 and 450 ns for 40- and 120-nm particles, respectively. These time scales are comparable with the 500-ns duration of soot oxidation observed in our two-laser study.[8]

In other experiments in our laboratory we found that polystyrene nanospheres and bulk solid exhibit similar temporal characteristics when irradiated at 193-nm; photofragmentation-fluorescence signals from both objects decay exponentially in about 10 ns.[33] However, a plasma was formed approximately at 10^9 W/cm^2 for the 100-nm nanospheres, while plasma formation was observed near 10^7 W/cm^2 from the bulk solid. Small particles interact differently with lasers than gas or bulk solids. Several researchers observed that the presence of particles in a gas reduced the optical breakdown threshold through intense laser vaporization of the particles followed by cascade collision ionization.[42–46] The breakdown of pure air by a 10.6-μm laser occurs at approximately 4×10^9 W/cm^2; the threshold decreases to 7×10^8 W/cm^2 for 3-μm NaCl particles in air.[43] The gas breakdown threshold is also a function of the particle size for these mixtures. The experimental and theoretical results by Lencioni[43] and Smith[46] showed that the breakdown threshold monotonically decreases with increasing particle diameter in the 1–20 μm range, and approaches the value corresponding to the laser-bulk solid interaction; e.g., 10^8 W/cm^2 for solid NaCl. As the particles become smaller, the threshold approaches that of a pure gas. Note that the absorption process, the particle size (or total number of atoms), and the chemical composition dictate the mode of photodecomposition of the particle surface and the behavior of the ejected species. Nanoparticles are photochemically disintegrated when irradiated by 193-nm photons at fluences of 10^7–10^9 W/cm^2. This distinguishes photofragmentation fluorescence from other spectroscopic techniques such as laser-induced incandescence (LII) and laser-induced breakdown spectroscopy (LIBS). LII often uses a pulsed laser of a longer wavelength, such as 532 or 1064 nm, with laser intensity of approximately 10^7 W/cm^2 to heat the particles.[37] On the other hand, the laser power in a LIBS experiment is usually greater than 10^9 W/cm^2, which produces a plasma plume where the temperature can be greater than 10 000 K, generating a continuum emission.[47]

B. Nanoparticle production

ArF laser irradiation at the lowest fluence (0.08 J/cm^2) with a single shot per particle in Fig. 3 produces a bimodal size distribution. The new peak created by laser irradiation is at approximately 20 nm and the number concentration of the distribution is 4.1×10^6 cm^{-3}. As the laser fluence increases, the peak diameter and concentration of the new mode of small particles also increase. These small particles are generated by photofragmentation of large agglomerates originally in the particle-laden flow with the total volume conserved. The absorbed photon energy is efficiently used to convert a portion of the particles into gas-phase atoms and molecules. After irradiation, the gaseous species undergo homogeneous nucleation to form new primary particles or interact with small fragments and primary particles, which may be released during photofragmentation, leading to heterogeneous nucleation (or surface growth). Agglomeration of the newly created primary particles and fragments also occurs. At a fluence of 0.08 J/cm^2, only a small fraction of the original particles is affected since there is not enough energy to completely fragment or dissociate every particle. As the fluence increases, a greater proportion of the particles is disintegrated into gaseous species and fragments. The higher concentration of the liberated species and fragments also promotes interactions among them. Agglomeration of the fragments, nucleation, and surface growth are all enhanced, resulting in an increase of the mean diameter and number concentration of the new small particles produced by photofragmentation. Similar phenomena were observed with polystyrene nanospheres in our laboratory. When monodisperse polystyrene nanospheres with a diameter of 100 nm were irradiated by 193-nm light, a new mode of smaller particles was generated; the smaller particles had a mean diameter near 20 nm and a number concentration an order of magnitude higher than the original particles. As the incident fluence increased, the mean size and number concentration of the new small particles also increased, suggesting that the new particles were produced by a similar process to that described above for NaCl particles.

These trends continue in the case of multiple laser shots in Fig. 4. The mean diameter grows from 27 to 55 nm and the number concentration increases from 7.9×10^6 to 1.8×10^7 cm^{-3} with eight laser shots striking each particle. There is more than 100 ms between each laser pulse. During

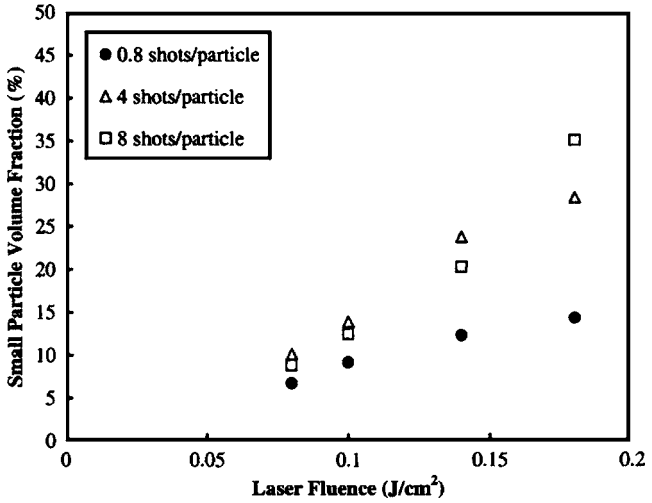

FIG. 8. Volume fraction of the new mode of small particles created by laser irradiation. The volume fraction is the ratio of the volume of new mode of particles smaller than the mean size (~118 nm) to that of the original, nonirradiated particles from the nebulizer system.

this time, the ejected gaseous species condense to form primary particles through nucleation and surface growth, and agglomeration further modifies the particle size distribution and morphology. Our two-laser study of NaCl particles confirmed that particle formation was completed within 500 μs. Once the particles reform after the first pulse, the second pulse photofragments the created particles. The particles go through another similar process of fragmentation and reforming.

Figure 8 shows the ratio of the volume of the small particles in Figs. 3 and 4 to the total volume of the distribution as a function of the laser fluence. The size distributions for 50 Hz are not presented in Figs. 3 and 4 since they are almost same as the 100-Hz case. The small particles are defined as the particles generated by photofragmentation that are smaller than the original mean diameter of the nonirradiated particles (118 nm). The volume fraction of the small particles monotonically increases with the laser fluence at all laser repetition rates. However, there is no significant difference (within the measurement uncertainty described earlier) when four or eight shots/particle are used; both produce about twice the volume fraction of small particles as the single shot case. Note that the incident photon energy is not enough to convert the entire particles into gas-phase species; small particles can be completely vaporized while a portion of large agglomerates is disintegrated into gaseous species.

When NaCl particles with an initial mean diameter of 26 nm are irradiated with a single laser pulse at 0.11 and 0.23 J/cm^2, the size distributions of the particles are very similar to the nonirradiated distribution (Fig. 7). The number of absorbed photons to the number of atoms in the particles (or photon/atom ratio) can be used to explain these results. For nanoscale particles, the photon/atom ratio is more relevant than the fluence because the absorption efficiency and total number of atoms are functions of particle size, and the number of available photons can limit the extent of particle disintegration. Table II shows the photon/atom ratios for various fluence conditions used in the present study. The ratios are calculated with the surface area and volume of the particles from SMPS results, assuming that all the photons striking the particles are absorbed. The photon/atom ratio (PAR) is useful in considering the energy balance for each particle and is inversely proportional to the particle mean diameter. The PARs are much higher for particles with a mean diameter of 26 nm than those of 118 nm. In addition, the absorption efficiency of 26-nm particles is more than an order of magnitude larger than 118-nm particles, suggesting that a majority of the particles originally with a mean diameter of 26 nm are likely converted into gas-phase species by 193-nm light. The gas-phase species recombine to form particulate matter whose distribution is similar to that of the nonirradiated particles since the condensation conditions are similar to where the particles were originally formed in the cooled region downstream of the tube furnace. If the particles were not completely vaporized by the laser, we would expect a mode of particles with a different size distribution, as observed previously in Figs. 3 and 4.

TABLE II. Photon-to-atom ratios (PARs) for various laser fluence conditions assuming that all the photons striking NaCl particles are absorbed.

Particles with a mean diameter of 118 nm	
0.08 J/cm^2	PAR=0.08
0.10 J/cm^2	PAR=0.10
0.14 J/cm^2	PAR=0.15
0.18 J/cm^2	PAR=0.20
Particles with a mean diameter of 26 nm	
0.11 J/cm^2	PAR=1.0
0.23 J/cm^2	PAR=2.0

C. NaCl versus carbonaceous particles

Photofragmentation of soot particles at 193 nm also produces a new mode of particles as shown in Fig. 6. When irradiated by a single laser pulse, the mean diameter of the small particles is similar to the primary particle size and the number concentration becomes one order of magnitude higher, similar to the results for the NaCl particles. However, when multiple laser shots are used, the mean diameter, number, and volume concentrations of the new particles are all reduced. The soot fragmentation species can oxidize, forming gaseous CO or CO_2. In addition, oxygen atoms or ozone generated by the 193-nm light in air can oxidize the carbon atoms on the particle surface. When the soot was irradiated in a N_2 environment, the particle loss was reduced.[7] The reactions of the liberated gaseous species and fragments is complete within 500 ns, as previously confirmed by our two-laser study of soot.[8] Successive laser pulses can vaporize more of the smaller soot particles, resulting in a loss of mass and a smaller mode of the observed particles. NaCl will not oxidize or react with oxygen or ozone, so the gas-phase species will recondense, forming larger particles as the fluence increases, with no loss of mass to stable gaseous species.

D. Particle morphology

In Fig. 5, the SEM images of the NaCl particles show a drastic change in particle morphology from 193-nm laser irradiation. The original particles have a fractal structure. Although we have not carried out a formal statistical analysis, the fractal dimension of the NaCl particles appears to be close to the value of combustion-generated particles, which is approximately 1.8. After irradiation, the agglomerates become less fractal and more spherical with a fractal dimension near 3. A number of SEM images (not shown) reveal that the irradiated particles have a smaller diameter and are present in a much larger number than the original particles, which is qualitatively consistent with SMPS results. In a majority of the spherical agglomerates, the shape of the primary particles is distinct, suggesting that they have not coalesced. A possible route of forming these spherical agglomerates is collision of the primary particles with the same charge. Although we do not see any broadband emission associated with plasma formation during photofragmentation, some ionization likely occurs. Thomson *et al.*[48] and Thomson and Murphy[49] estimated that the ion formation threshold for 193-nm laser irradiation in vacuum is near the fluence used in this study. The partial ionization can make a portion of the formed primary particles charged. These charged primary particles undergo a collision process, forming spherical clusters. This process is called Eden growth, which occurs through the primary particle-cluster aggregation in a reaction-limited regime.[50–52] Similar phenomena were observed in photofragmentation of combustion-generated soot.[7] Laser irradiation of soot particles at 100 Hz produced a few ~ 1 μm spherical clusters as well as a large number of small spherical particles. The size and spherical shape of the irradiated particles confirm that particles are certainly disintegrated by photofragmentation and reformed, suggesting that 193-nm light irradiation can control particle size and morphology and be possibly useful for nanoparticle technology.

V. CONCLUSIONS

The interaction of NaCl nanoparticles with 193-nm light is studied to gain understanding of particle disintegration and production by UV photofragmentation. Irradiation of the particles by 193-nm photons with the fluence of $0.08-0.18$ J/cm^2 at 10 and 100 Hz produces a new mode of particles with a smaller mean diameter and a number concentration higher than the original particles. The mean diameter of the irradiated particles increases from 20 to 55 nm, and the number concentration of particles increases from 4.1×10^6 to 1.8×10^7 cm^{-3} over the laser conditions studied.

During the laser pulse, a portion of the original particles is disintegrated into gas-phase species depending on the photon energy density. The ejected gaseous species recondense to new primary particles through homogeneous nucleation and surface growth on the fragments released by photofragmentation. Agglomeration of the newly created primary particles and the fragments further modifies the size distribution and morphology. The mean diameter, number, and volume of the small particles created by irradiation monotonically increase with the incident laser fluence. The concept of the number of photon to the number of atoms in the particles (photon/atom ratio) is introduced to analyze the extent of particle disintegration by UV photons. In the case of the carbon-based particles, the volume of the particles is lost by oxidation of gas-phase species generated by intense UV photon irradiation. Loss of particle volume by successive photofragmentation reduces the mean diameter and number concentration.

SEM images qualitatively show the modification of the particle size and morphology by laser irradiation. The original, nonirradiated particles are fractal in shape, while the irradiated particles become spherical clusters composed of the primary particles. In conclusion, the particle disintegration and production processes are analyzed for photofragmentation in laser-based particle measurements and this technique could be used for size and morphology control of nanoparticles.

ACKNOWLEDGMENTS

This work was supported by the Environmental Health Sciences Superfund Basic Research Program (Grant No. P42ESO47050-01) from the National Institute of Environmental Health Sciences, NIH, with funding provided by the EPA. Its contents are solely the responsibility of the authors and do not necessarily represent the official views of NIEHS, NIH, or EPA.

[1] D. T. Suess and K. A. Prather, Chem. Rev. (Washington, D.C.) **99**, 3007 (1999).
[2] M. F. Becker, J. R. Brock, H Cai, D. E. Henneke, J. W. Keto, J. Lee, W. T. Nichols, and H. D. Glicksman, Nanostruct. Mater. **10**, 853 (1998).
[3] H Cai, N. Chauhary, J. Lee, M. F. Becker, J. R. Brock, and J. W. Keto, J. Aerosol Sci. **29**, 627 (1998).
[4] H. Kurita, A. Takami, and S. Koda, Appl. Phys. Lett. **72**, 789 (1998).
[5] F. Mafune, J. Kohno, Y. Takeda, and T. Kondow, J. Phys. Chem. **105**, 9050 (2001).
[6] C. J. Damm, D. Lucas, R. F. Sawyer, and C. P. Koshland, Appl. Spectrosc. **55**, 1478 (2001).
[7] C. B. Stipe, J. H. Choi, D. Lucas, C. P. Koshland, and R. F. Sawyer, J. Nanopart. Res. **6**, 467 (2004).
[8] C. B. Stipe, D. Lucas, C. P. Koshland, and R. F. Sawyer, Appl. Opt. (to be published).
[9] D. R. Lide, *CRC Handbook of Chemistry and Physics* (CRC, New York, 1998).
[10] E. D. Palik, *Handbook of Optical Constants of Solids* (Academic, Orlando, FL, 1985).
[11] P. E. Dyer, S. M. Maswadi, and C. D. Walton, Appl. Phys. A: Mater. Sci. Process. **76**, 817 (2003).
[12] P. E. Dyer and C. D. Walton, Appl. Phys. A: Mater. Sci. Process. **79**, 721 (2004).
[13] Y. Kawaguchi, M. L. Dawes, S. C. Langford, and J. T. Dickinson, J. Appl. Phys. **89**, 2370 (2001).
[14] M. H. Nunez and N. Omenetto, Appl. Spectrosc. **55**, 809 (2001).
[15] R. L. Webb, L. C. Jensen, S. C. Langford, and J. T. Dickinson, J. Appl. Phys. **74**, 2338 (1993).
[16] B. L. Chadwick, G. Domazetis, and R. J. S. Morrison, Anal. Chem. **67**, 710 (1995).
[17] K. T. Hartinger, P. B. Monkhouse, and J. Wolfrum, in *25th Symposium (International) on Combustion*, July 31–August 5, 1994, Sapporo, Japan (The Combustion Institute, Pittsburgh, PA, 1994).
[18] R. C. Oldenborg and S. L. Baughcum, Anal. Chem. **58**, 1430 (1986).
[19] J. B. Simeonsson and R. C. Sausa, Appl. Spectrosc. Rev. **31**, 1 (1996).
[20] H. G. Scheibel and J. Porstendorfer, J. Aerosol Sci. **14**, 113 (1983).
[21] W. C. Hinds, *Aerosol Technology Properties, Behavior, and Measurement of Airborne Particles* (Wiley, New York, 1982).
[22] G. J. Smallwood *et al.*, SAE Technical Paper No. 2002-01-2715 (2002), p. 1.

[23]C. F. Bohren and D. R. Huffman, *Absorption and Scattering of Light by Small Particles* (Wiley Interscience, New York, 1983).
[24]K. M. Beck, A. G. Joly, N. F. Dupuis, W. P. Hess, P. V. Sushko, and A. L. Shluger, J. Chem. Phys. **120**, 2456 (2004).
[25]W. P. Hess, A. G. Joly, K. M. Beck, P. V. Sushko, and A. L. Shluger, Surf. Sci. **564**, 62 (2004).
[26]D. B. Sirdeshmukh, L. Sirdeshmukh, and K. G. Subhadra, *Alkali Halides: A Handbook of Physical Properties* (Springer, New York, 2001).
[27]D. Bauerle, *Laser Processing and Chemistry* (Springer, Heidelberg, 2000).
[28]*Desorption Induced by Electronic Transitions DIET I* edited by N. H. Tolk, M. M. Traum, J. C. Tully, and T. E. Madey (Springer, New York, 1983).
[29]H. W. Etzel and D. A. Patterson, Phys. Rev. **112**, 1112 (1958).
[30]B. J. Garrison and R. Srinivasan, Appl. Phys. Lett. **44**, 849 (1984).
[31]X. Li, R. D. Beck, and R. L. Whetten, Phys. Rev. Lett. **68**, 3420 (1992).
[32]W. P. Hess, A. G. Joly, K. M. Beck, D. P. Gerrity, P. V. Sushko, and A. L. Shluger, Appl. Phys. Lett. **81**, 1140 (2002).
[33]J. H. Choi, C. P. Koshland, R. F. Sawyer, and D. Lucas, Appl. Spectrosc. (submitted).
[34]C. J. Damm, D. Lucas, R. F. Sawyer, and C. P. Koshland, in *29th Symposium (International) on Combustion*, July 21–26, 2002, University of California, Irvine, CA. (The Combustion Institute, Pittsburgh, PA, 2002).
[35]K. Knutsen and T. M. Orlando, Phys. Rev. B **55**, 13246 (1997).
[36]K. Knutsen and T. M. Orlando, Appl. Surf. Sci. **127–129**, 1 (1998).
[37]H. A. Michelsen, J. Chem. Phys. **118**, 7012 (2003).
[38]E. Sutcliffe and R. Srinivasan, J. Appl. Phys. **60**, 3315 (1986).
[39]R. Srinivasan, J. Appl. Phys. **73**, 2743 (1993).
[40]D. J. Krajnovich, J. Chem. Phys. **102**, 726 (1995).
[41]J. K. Oman and S. J. Garrett, J. Phys. Chem. B **106**, 10417 (2002).
[42]P. Chylek, M. A. Jarzembski, V. Srivastava, and R. G. Pinnick, Appl. Opt. **29**, 2303 (1990).
[43]D. E. Lencioni, Appl. Phys. Lett. **23**, 12 (1973).
[44]R. G. Pinnick, A. Biswas, R. L. Armstrong, S. G. Jennings, J. D. Pendleton, and G. Fernandez, Appl. Opt. **29**, 918 (1990).
[45]D. Smith, Appl. Phys. Lett. **19**, 405 (1971).
[46]D. Smith, J. Appl. Phys. **48**, 2217 (1977).
[47]D. W. Hahn and M. M. Lunden, Aerosol Sci. Technol. **33**, 30 (2000).
[48]D. S. Thomson, A. M. Middlebrook, and D. M. Murphy, Aerosol Sci. Technol. **26**, 544 (1997).
[49]D. S. Thomson and D. M. Murphy, Appl. Opt. **32**, 6818 (1993).
[50]Y. V. Ivanenko, N. I. Lebovka, and N. V. Vygornitskii, Eur. Phys. J. B **11**, 469 (1999).
[51]D. W. Schaefer, MRS Bull. **13**, 22 (1988).
[52]D. W. Schaefer and A. J. Hurd, Aerosol Sci. Technol. **12**, 876 (1990).